THE JOURNAL OF BIOLOGICAL CHEMISTRY VOL. 287, NO. 47, pp. 39898–39910, November 16, 2012

Regulation of Autophagy and Its Associated Cell Death by "Sphingolipid Rheostat"

RECIPROCAL ROLE OF CERAMIDE AND SPHINGOSINE 1-PHOSPHATE IN THE MAMMALIAN TARGET OF RAPAMYCIN PATHWAY[*][S]

Received for publication, September 4, 2012, and in revised form, October 2, 2012 Published, JBC Papers in Press, October 3, 2012, DOI 10.1074/jbc.M112.416552

Makoto Taniguchi[‡§], Kazuyuki Kitatani[‡¶], Tadakazu Kondo[‖], Mayumi Hashimoto-Nishimura[‡], Satoshi Asano[‡**], Akira Hayashi[‡‡¶¶], Susumu Mitsutake[‖‖], Yasuyuki Igarashi[‖‖], Hisanori Umehara[¶¶], Hiroyuki Takeya[‡‡], Junzo Kigawa[**], and Toshiro Okazaki[‡¶¶¹]**

*From the [‡]Division of Clinical Laboratory Medicine, Faculty of Medicine, the **Tottori University Hospital Cancer Center, and the [‡‡]Division of Pathological Biochemistry, Department of Biomedical Science, Faculty of Medicine, Tottori University, 86 Nishi-Machi, Yonago 683-8503, the [§]Department of Life Science, Medical Research Institute, Kanazawa Medical University, 1-1 Daigaku Uchinada, Ishikawa 920-0293, the [¶]Department of Biobank, Tohoku Medical Megabank Organization, Tohoku University, 1-1 Seiryo, Aoba, Sendai 980-8574, the [‖]Department of Hematology and Oncology, Graduate School of Medicine, Kyoto University, 54 Shogoin Kawaharacho Sakyo-ku, Kyoto 606-8507, the [¶¶]Department of Hematology and Immunology, Kanazawa Medical University, 1-1 Daigaku Uchinada, Ishikawa 920-0293, and the [‖‖]Laboratory of Biomembrane and Biofunctional Chemistry, Faculty of Advanced Life Sciences, Hokkaido University, Kita 21-jo, Nishi 11-choume, Kita-ku, Sapporo 001-0021, Japan*

Background: The sphingolipids ceramide and sphingosine 1-phosphate (S1P) control various cellular functions, including proliferation, cell death, and autophagy.
Results: Binding of S1P to its receptor $S1P_3$ counteracts ceramide-mediated autophagy by activating the mammalian target of rapamycin (mTOR) pathway.
Conclusion: Sphingolipid rheostat between ceramide and S1P plays an important role in regulating mTOR-controlled autophagy.
Significance: We provide new insights into novel regulatory mechanisms in autophagy induction.

The role of "sphingolipid rheostat" by ceramide and sphingosine 1-phosphate (S1P) in the regulation of autophagy remains unclear. In human leukemia HL-60 cells, amino acid deprivation (AA(−)) caused autophagy with an increase in acid sphingomyleinase (SMase) activity and ceramide, which serves as an autophagy inducing lipid. Knockdown of acid SMase significantly suppressed the autophagy induction. S1P treatment counteracted autophagy induction by AA(−) or C_2-ceramide. AA(−) treatment promoted mammalian target of rapamycin (mTOR) dephosphorylation/inactivation, inducing autophagy. S1P treatment suppressed mTOR inactivation and autophagy induction by AA(−). S1P exerts biological actions via cell surface receptors, and $S1P_3$ among five S1P receptors was predominantly expressed in HL-60 cells. We evaluated the involvement of $S1P_3$ in suppressing autophagy induction. S1P treatment of CHO cells had no effects on mTOR inactivation and autophagy induction by AA(−) or C_2-ceramide. Whereas S1P treatment of $S1P_3$ overexpressing CHO cells resulted in activation of the mTOR pathway, preventing cells from undergoing autophagy induced by AA(−) or C_2-ceramide. These results indicate that S1P-$S1P_3$ plays a role in counteracting ceramide signals that mediate mTOR-controlled autophagy. In addition, we evaluated the involvement of ceramide-activated protein phosphatases (CAPPs) in ceramide-dependent inactivation of the mTOR pathway. Inhibition of CAPP by okadaic acid in AA(−)- or C_2-ceramide-treated cells suppressed dephosphorylation/inactivation of mTOR, autophagy induction, and autophagy-associated cell death, indicating a novel role of ceramide-CAPPs in autophagy induction. Moreover, $S1P_3$ engagement by S1P counteracted cell death. Taken together, these results indicated that sphingolipid rheostat in ceramide-CAPPs and S1P-$S1P_3$ signaling modulates autophagy and its associated cell death through regulation of the mTOR pathway.

Sphingolipids characterized with the presence of sphingoid bases are a family of membrane lipids, such as ceramide, glucosylceramide, sphingomyelin, sphingosine, and sphingosine 1-phosphate (S1P)[2] (1–4). A number of sphingolipids are

* This work was supported in part by grants from the Sapporo Biocluster "Bio-S," the Knowledge Cluster Initiative of the Ministry of Education, Culture, Sports, Science and Technology (Japan), the Japan Society for the Promotion of Science (Grant-in-Aid for Young Scientists 21890144) (to K. K.), the Sumitomo Foundation (to K. K.), the Japanese Ministry of Education, Culture, Sports, Science and Technology 22249041 (to H. U.), the Uehara Memorial Foundation (to H. U.), the Vehicle Racing Commemorative Foundation (to H. U.), and the Kanazawa Medical University Research Foundation (to H. U).
[S] This article contains supplemental Figs. S1 and S2.
[1] To whom correspondence should be addressed: Dept. of Medicine, Division of Hematology/Immunology, Kanazawa Medical University, 1-1 Daigaku, Uchinada, Ishikawa 920-0293, Japan. Tel.: 81-76-218-8337; Fax: 81-76-286-9290; E-mail: toshiroo@kanazawa-med.ac.jp.

[2] The abbreviations used are: S1P, sphingosine-1-phosphate; C_2-ceramide, *N*-acetylsphingosine; AA(−), amino acid deprivation; mTOR, mammalian target of rapamycin; p70 S6K, the 70-kDa ribosomal protein S6 kinase; 4E-BP1, eukaryotic initiation factor 4-binding protein 1; LC3, microtubule-associated protein-1 light chain-3; CAPPs, ceramide-activated protein phosphatases; MDC, monodansylcadaverine; 3-MA, 3-methyladenine; SMase, sphingomyleinase; SMS, sphingomyelin synthase; q-RT, quantitative RT.

emerging as bioactive lipids thought to play crucial roles in cellular responses including inflammation, cell proliferation, differentiation, apoptosis, cell migration, senescence, and autophagy (5–8).

Ceramide initially emerged as a lipid mediator of apoptotic cell death, and many molecules including cathepsin D, ceramide-activated protein phosphatases (CAPPs), and PKCζ were shown to be involved in its signaling (9–11). Ceramide was also reported to promote the formation of autophagic vacuoles by up-regulating beclin 1 (12) and to play a role in regulating autophagy and its associated cell death (13–15). However, the molecular mechanism by which ceramide modulates autophagy signaling has not been elucidated fully.

S1P is formed by the sequential catalytic metabolism of ceramide. Ceramidase degrades ceramide to form sphingosine, which in turn is converted to S1P by sphingosine kinase (3, 16). Extrinsic S1P is involved in highly diverse cellular functions including adherent junction assembly, cytoskeleton changes, cell migration and proliferation through specific G protein coupled-membrane receptors ($S1P_{1-5}$) (17–22). Interestingly, S1P intrinsically targets specific intracellular proteins and exerts biological responses independently of S1P receptors (23). In terms of autophagy, overexpression of sphingosine kinase 1 was reported to induce autophagy independently of Akt/protein kinase B in MCF-7 cells (24). Furthermore, Lépine *et al.* (25) showed that deletion of sphingosine-1-phosphate phosphohydrase-1, which is a metabolic enzyme of S1P, induces autophagy without the involvement of the mammalian target of rapamycin (mTOR) and type III phosphoinositide 3 (PI3)-kinase-beclin-1 pathways. That study demonstrates that intrinsic, but not extrinsic, S1P serves as an inducing lipid. However, recent studies have shown that extrinsic S1P activates the mTOR pathway through S1P receptors (26–28), and it was assumed that extrinsic S1P counteracts autophagy induction by activating its receptor-mTOR pathway.

S1P and ceramide are biologically interconvertible lipids (8), and it has been proposed that their relative levels determine cell fate (*i.e.* life or death) (29, 30). The relevance of this "sphingolipid rheostat" in regulating cell fate has been demonstrated in many different cell types (31). In the present study, we demonstrate that the sphingolipid rheostat also modulates autophagy.

EXPERIMENTAL PROCEDURES

Materials—S1P and *N*-acetylsphingosine (C_2-ceramide) were purchased from Matreya (Pleasant Gap, PA). Monodansylcadaverine (MDC), rapamycin, 3-methyladenine (3-MA), and myriosin were obtained from Sigma. Fumonisin B1 and okadaic acid were from Merck Millipore (Darmstadt, Germany). CAY10444 was purchased from Cayman Chemical (Ann Arbor, MI). 4′,6-Diamidino-2-phenylindole (DAPI) was from Roche Applied Science. The rabbit polyclonal anti-microtubule-associated protein-1 light chain-3 (LC3) antibody was from MBL (Nagoya, Japan). The rabbit polyclonal anti-eukaryotic initiation factor 4-binding protein 1 (4E-BP1) antibody was from Santa Cruz Biotechnology (Santa Cruz, CA). The rabbit polyclonal anti-mTOR, anti-phospho-mTOR (Ser-2448), anti-p70 S6K, anti-phospho-p70 S6K (Tyr-389), anti-phospho-4E-BP1 (Thr-37/46) antibodies were from Cell Signaling (Danvers, MA). Horseradish peroxidase-conjugated secondary antibodies were obtained from Promega (Madison, WI).

Cell Culture and Autophagy Induction—Human leukemia HL-60 cells were cultured in RPMI 1640 medium containing 10% (v/v) fetal calf serum (FCS). Autophagy was induced by amino acid deprivation (AA(−)). Cells were washed three times with phosphate-buffered saline (PBS) and incubated with amino acid (L-glutamine, L-leucine, L-lysine, L-methionine)-free RPMI1640 medium (Nissui, Tokyo, Japan) in the absence of FCS at 37 °C in a humidified atmosphere containing 5% CO_2. Chinese hamster ovary (CHO) and CHO/$S1P_3$ cells were cultured in α-minimal essential medium containing 10% (v/v) FCS (32). For autophagy induction, CHO cells were incubated in serum-free α-minimal essential medium for 3 h, and then the medium was replaced with AA(−) medium.

Electron Microscopy—After treatment, cells were harvested, washed twice with PBS, and fixed with 2.5% (w/v) glutaraldehyde in PBS. Fixed cells were treated with 1% (w/v) osmium tetraoxide in PBS and dehydrated in ethanol, followed by epoxy-1,2-propane treatment. Ultrathin sections obtained with a diamond knife were counterstained with uranyl acetate in ethanol solution, followed by lead citrate. Images were collected with a CCD camera.

Labeling of Autophagic Vacuoles with MDC—Cells were incubated with 50 μM MDC (33) in PBS at 37 °C for 10 min following autophagy induction. After incubation, the cells were washed three times with PBS, placed on glass slides by cytospinning and immediately analyzed by fluorescence microscopy using an inverted microscope equipped with a filter system. Images were obtained with a CCD camera and processed using the program Cool Snap (Roper Industries, Sarasota, FL). MDC incorporated into cells was expressed as the fluorescence intensity (arbitrary units) per one cell, and at least 200 cells were calculated by the program MacSCOPE (Mitani, Fukui, Japan).

Ceramide Measurements—After extracting lipids according to the Bligh and Dyer method (34, 35), ceramide levels were determined by the diacylglycerol kinase assay using [γ-^{32}P]ATP and *Escherichia coli* diacylglycerol kinase, which converts ceramide and diacylglycerol to ceramide 1-phosphate and phosphatidic acid, respectively (35). Radioactivity of ceramide corresponding to ceramide 1-phosphate was detected and quantified with the BAS-2000 (Fujifilm, Tokyo, Japan). Amounts of ceramide were normalized with phospholipid phosphate.

Acid and Neutral Sphingomyelinase (SMase) Activities—Cells were lysed in ice-cold lysis buffer (10 mM Tris-HCl, pH 7.5, 1 mM EDTA, 0.1% Triton X-100, 1 mM phenylmethylsulfonyl fluoride, 2.5 μg/ml of leupeptin, and 2.5 μg/ml of aprotinin). The assay mixture for the measurement of acid SMase contained 0.1 M sodium acetate (pH 5.0), 10 μM C_6-NBD-sphingomyelin, 0.1% Triton X-100, and 100 μg of total protein. The reaction mixture for magnesium-dependent neutral SMase contained 0.1 M Tris-HCl (pH 7.5), 10 μM C_6-NBD-sphingomyelin, 10 mM $MgCl_2$, 0.1% Triton X-100, 5 mM dithiothreitol, and 100 μg of lysate. Incubation was carried out at 37 °C for 90 min. Lipids were extracted using the Bligh and Dyer method (34), applied onto TLC plates and developed with a solvent consisting of chloroform, methanol, 12 mM $MgCl_2$ (65:25:4, v/v/v). The

TABLE 1
Sequence of siRNAs used in this study

siRNA	Sense/antisense	5′ → 3′
SMPD1-a	Sense	GCCCUGCCGUCUGGCUACUCUUUGU
	Antisense	ACAAAGAGUAGCCAGACGGCAGGGC
SMPD1-b	Sense	GAGCUGGAAUUAUUACCGAAUUGUA
	Antisense	UACAAUUCGGUAAUAAUUCCAGCUC

fluorescent lipids were visualized using LAS-1000 plus (Fujifilm, Japan) and quantified using MultiGauge 3.1 (Fujifilm).

Sphingomyelin Synthase (SMS) Activity—HL-60 cells were homogenized in ice-cold buffer (20 mM Tris-HCl, pH 7.4, 2 mM EDTA, 10 mM EGTA, 1 mM phenylmethylsulfonyl fluoride, 2.5 μg/ml of leupeptin, and 2.5 μg/ml of aprotinin), and 100 μg of total protein was mixed with the reaction solution (10 mM Tris-HCl, pH 7.5, 1 mM EDTA, 20 μM C_6-NBD-ceramide, 120 μM phosphatidylcholine) and incubated at 37 °C for 90 min.

Transfection with Small Interfering RNA (siRNA)—Cells were transfected with 40 nM double-strand siRNAs for scrambled sequence or acid SMase using MultiFectam (Promega) according to the manufacturer's instructions. After 72 h, cells were washed and treated with AA(+) or AA(−) to induce autophagy. Table 1 shows sequences of acid SMase siRNA.

Western Blot Analysis—Cells were harvested, washed twice with PBS, and resuspended in lysis buffer containing 10 mM Tris-HCl (pH 7.4), 10 mM KCl, 1.5 mM $MgCl_2$, 1% (v/v) Triton X-100, 1 mM phenylmethylsulfonyl fluoride, 10 μg/ml of leupeptin, and 10 μg/ml of aprotinin. After being left on ice for 30 min, the lysates were centrifuged at 10,000 × *g* for 15 min at 4 °C. Supernatant proteins (50 μg) were electrophoresed on a 10% (w/v) SDS-polyacrylamide gel, and transferred to polyvinylidene difluoride membrane (Millipore, Bedford, MA). The membrane was blocked with PBS containing 5% (w/v) skim milk and 0.1% (v/v) Tween 20 for 1 h at room temperature and then incubated with antibodies for phospho-mTOR, 4E-BP-1, phospho-4E-BP-1, p70 S6K, phospho-p70 S6K, or LC3 antibodies for 1 h. After three washes with PBS containing 0.1% (v/v) Tween 20, the membrane was incubated with horseradish peroxidase-conjugated secondary antibody for 1 h. After washing, protein detection was performed using ECL Western blotting detection reagents (Amersham Biosciences) according to the manufacturer's protocol. Bands were quantified with ImageJ 1.43.

Immunoprecipitation and in Vitro Kinase Activity of mTOR—HL-60 cells (3×10^7) were rinsed twice with cold PBS and lysed on ice for 20 min in lysis buffer (40 mM HEPES, pH 7.5, 120 mM NaCl, 1 mM EDTA, 10 mM pyrophosphate, 10 mM β-glycerophosphate, 50 mM sodium fluoride, EDTA-free protease inhibitors, and 0.3% (v/v) CHAPS). After centrifugation at 13,000 × *g* for 10 min, 10 μg of mTOR antibody was added to the supernatants. After rotation for 4 h, 20 ml of 50% (v/v) slurry of protein G-Sepharose (Amersham Biosciences) was then added to the supernatants followed by a further incubation for 2 h. Captured immunoprecipitates were washed four times with lysis buffer and once with wash buffer (50 mM HEPES, pH 7.5, 40 mM NaCl, and 2 mM EDTA). Immunoprecipitates were submitted to Western blot analysis. In *in vitro* mTOR kinase assays, immunoprecipitants were incubated with substrates (1 μg of recombinant 4E-BP1 or recombinant p70 S6 kinase) at 30 °C for 40 min in buffer containing 10 mM HEPES (pH 7.4), 50 mM β-glycerophosphate, 50 mM NaCl, 200 nM microcystin-LR, 10 μg/ml of leupeptin, 5 μg/ml of aprotinin, 5 μg/ml of pepstatin A, 600 μM phenylmethylsulfonyl fluoride, 1 mM sodium orthovanadate, 10 μCi of [γ-^{32}P]ATP, and 200 μM ATP. After electrophoresis in SDS-polyacrylamide gels, phosphorylated proteins were visualized by autoradiography.

Reverse Transcriptase-Polymerase Chain Reaction (RT-PCR) and Quantitative Real-time PCR (Q-RT-PCR)—RNAs were extracted using an RNA purification kit (RNeasy, Qiagen, Hilden, Germany), and 5 μg of total RNA was converted to complementary DNA (cDNA) using the cDNA synthesis kit (TaKaRa Shuzo Co., Kyoto, Japan). cDNAs were amplified using the Premix TaqPCR kit (TaKaRa) in a PCR thermal cycler. The following primer sets were used: for glyceraldehydes-3-phosphate dehydrogenase (GAPDH), forward 5′-AAGGCTGTGGGCAAGGTCAT-3′ and reverse 5′-CACCACCCTGTTGCTGTAGC-3′; for human $S1P_1$, forward 5′-CCAGCGTCCCGCTGGTCAAG-3′ and reverse 5′-ACCCAGCAGGCGCTGATTAG-3′; for human $S1P_2$, forward 5′-AGTACCTGAACCCCAACAAGG-3′ and reverse 5′-GTCACCACGCACAGCACATAA-3′; for human $S1P_3$, forward 5′-TGGAGCTAATCGTCTGTGAATGC-3′ and reverse 5′-GTGAAGGCAATGAGCCAGCACA-3′; for human $S1P_4$, forward 5′-GCTCATTGTTCTGCACTACAACCA-3′ and human reverse 5′-AAGGCTGGAGCAGCGGTCAAAG-3′; for human $S1P_5$, forward 5′-GTTGTTGGTGCTCGGACGCCAC-3′ and human reverse 5′-TGCGCGCGTAGAGTGCACAGAT-3′. PCR products were separated on a 5% (w/v) polyacrylamide gel and detected with ethidium bromide staining.

Q-RT-PCR was performed using an Applied Biosystems 7300 Real-time PCR System, according to the standard TaqMan PCR kit protocol. TaqMan probes of S1P receptors were purchased from Applied Biosystems. The GAPDH was used as an internal reference control to normalize relative levels of mRNA expression.

Constructs and Transfection—The tandem mRFP-GFP-tagged LC3 (tfLC3) vector (36) was a kind gift from Dr. Yoshimori (Osaka University, Osaka, Japan). CHO cells were transfected with TransIT-LT1 (Mirus Bio Corporation, WI). After 12 h transfection, cells were seeded on poly-L-lysine-coated glass coverslips and used for assays.

Confocal Microscopy—For endogenous LC3 detection, cells were cultured at various conditions, washed twice with cold PBS, and attached onto glass slides by cytospinng. Cells were fixed with 1% (w/v) paraformaldehyde for 15 min at 4 °C and permeabilized with 0.1% (v/v) Triton X-100 for 5 min at room temperature. Cells were then blocked with PBS containing 2% (w/v) BSA and 0.1% (v/v) Tween 20 for 20 min and treated with anti-LC3 antibody for 90 min at room temperature. Cells were washed five times and treated with anti-mouse IgG Alexa Fluor 488. Images were obtained by confocal microscopy using the Leica TSC SP2 (Leica microsystems, Wetzlar, Germany).

Detection Autophagic Flux Using RFP-GFP-LC3—The CHO/$S1P_3$ cells were transiently transfected with tfLC3 vector, and treated with various conditions after 24 h transfection. Cells were washed twice with cold PBS and fixed with 2% (w/v) para-

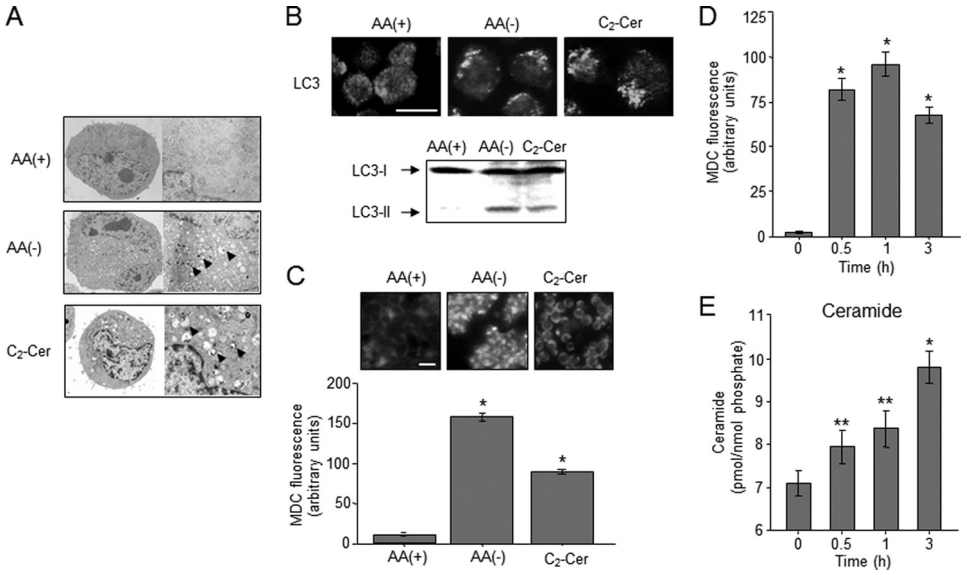

FIGURE 1. **Autophagy and ceramide accumulation induced by amino acid deprivation (AA(−)) in human leukemia HL-60 cells.** *A,* HL-60 cells were incubated in medium containing amino acids (AA(+)) or medium without amino acids (AA(−)). For ceramide treatment, cells were incubated with 10 μM C_2-ceramide (C_2-Cer) for 1 h in AA(+) medium. Morphological changes were detected by electron microscopy. *Arrowheads* indicate autophagosome formation. *B,* cells were treated with AA(+), AA(−), and C_2-Cer for 1 h. *Upper panel*, LC3 protein was detected by immunoblotting. *Right panel*, autophagosome formation was detected with immunocytochemistry using the anti-LC3 antibody. *Scale bar*, 10 μm. *C*, after treatment of cells with AA(+), AA(−), or C_2-Cer, cells were further incubated with 50 μM MDC for 10 min and immediately analyzed by fluorescence microscopy. The density of MDC was assessed by the program MacSCOPE. *Scale bar*, 10 μm. *, $p < 0.005$ *versus* AA(+). *D,* cells were treated with AA(−) medium for the indicated time periods. Then autophagy was measured by MDC incorporation. *E,* ceramide content was determined by the diacylglycerol kinase assay after lipid extraction by the Bligh and Dyer (34) method as described under "Experimental Procedures." Values are the mean ± S.D. from three independent experiments. *, $p < 0.005$ *versus* 0 h; **, $p < 0.05$ *versus* 0 h.

formaldehyde for 20 min at 4 °C. Images were gained with fluorescent microscopy (Nikon Instruments Inc., NY).

Determination of Serine/Threonine Protein Phosphatase Activity—Cells were harvested and treated with the hypotonic buffer containing 10 mM HEPES-KOH (pH 7.4), 10 mM KCl, and 2 mM $MgCl_2$ for 30 min on ice. The swollen cells were homogenized using a 27-gauge needle, and the cell lysates were centrifuged at 10,000 × *g* for 10 min at 4 °C. The supernatants (0.3 μg of protein) were used for serine/threonine protein phosphatase assay. The proteins were incubated with or without 500 nM okadaic acid prior to performing the measurement of serine/threonine protein phosphatase activity using a ProFluor®Ser/Thr PPase assay kit (Promega). The protein phosphatase activity insensitive to okadaic acid was subtracted from a okadaic acid-sensitive one, giving specific PP1/PP2A activity.

DAPI Staining—Cells were harvested and then fixed in 1% (w/v) paraformaldehyde for 30 min at room temperature, followed by DAPI staining as described previously (37). At least 200 cells were counted under a fluorescent microscope, and cells with nuclear condensation and fragmentation were designated as dead cells.

Statistical Analysis—Comparisons between two groups were carried out using the unpaired Student's *t* test.

RESULTS

AA(−) Induces Autophagy Concomitant with Ceramide Accumulation in Human Leukemia HL-60 Cells—AA(−) promotes autophagy in many cell types such as liver, breast, and colon cancer cells (38–40). Autophagy begins with the formation of double-membrane autophagosomes that engraft cytoplasmic proteins and suborganelles. The autophagosomes are fused to lysosomes for bulk degradation. Herein, we showed that human leukemia HL-60 cells also underwent autophagy in response to AA(−) (Fig. 1. Electron microscopy revealed that AA(−) medium-cultured HL-60 cells were generated a myriad of vacuoles like autophagosomes, whereas no significant detection of autophagosomes was observed in regular AA(+) medium-cultured cells (Fig. 1*A*). Autophagosome formation and progressive fusion to lysosomes are mediated by converting LC3 from a cytosolic form (LC3-I) to a phosphatidylethanolamine-conjugated membrane-bound form (LC3-II) (41). The cellular localization of the autophagy-related protein LC3 changes from a diffuse cytosolic pattern to a punctate pattern during autophagy (41). The formation of LC3 puncta (immunofluorescence) and LC3-II (immunoblotting) was promoted in response to AA(−) (Fig. 1*B*). Autophagy is also characterized by the incorporation of MDC as previously described (33), and MDC incorporation was significantly increased after AA(−) treatment (Fig. 1*C*). Similar to AA(−), autophagy was also induced in response to the cell permeable C_2-ceramide (Figs. 1, *A–C*), which is a known autophagy-inducing lipid (12, 15).

Ceramide was assumed to mediate autophagy induction following AA(−) treatment. To assess the effects of AA(−) on ceramide accumulation, ceramide levels were determined using the diacylglycerol kinase assay. Accompanied with an increase in MDC incorporation (Fig. 1*D*), ceramide was significantly accumulated in a time-dependent manner after exposure of cells to AA(−) (Fig. 1*E*). This increase in ceramide declined to baseline levels with AA(+), when AA(−) conditions were restored by the addition of amino acids (data not shown).

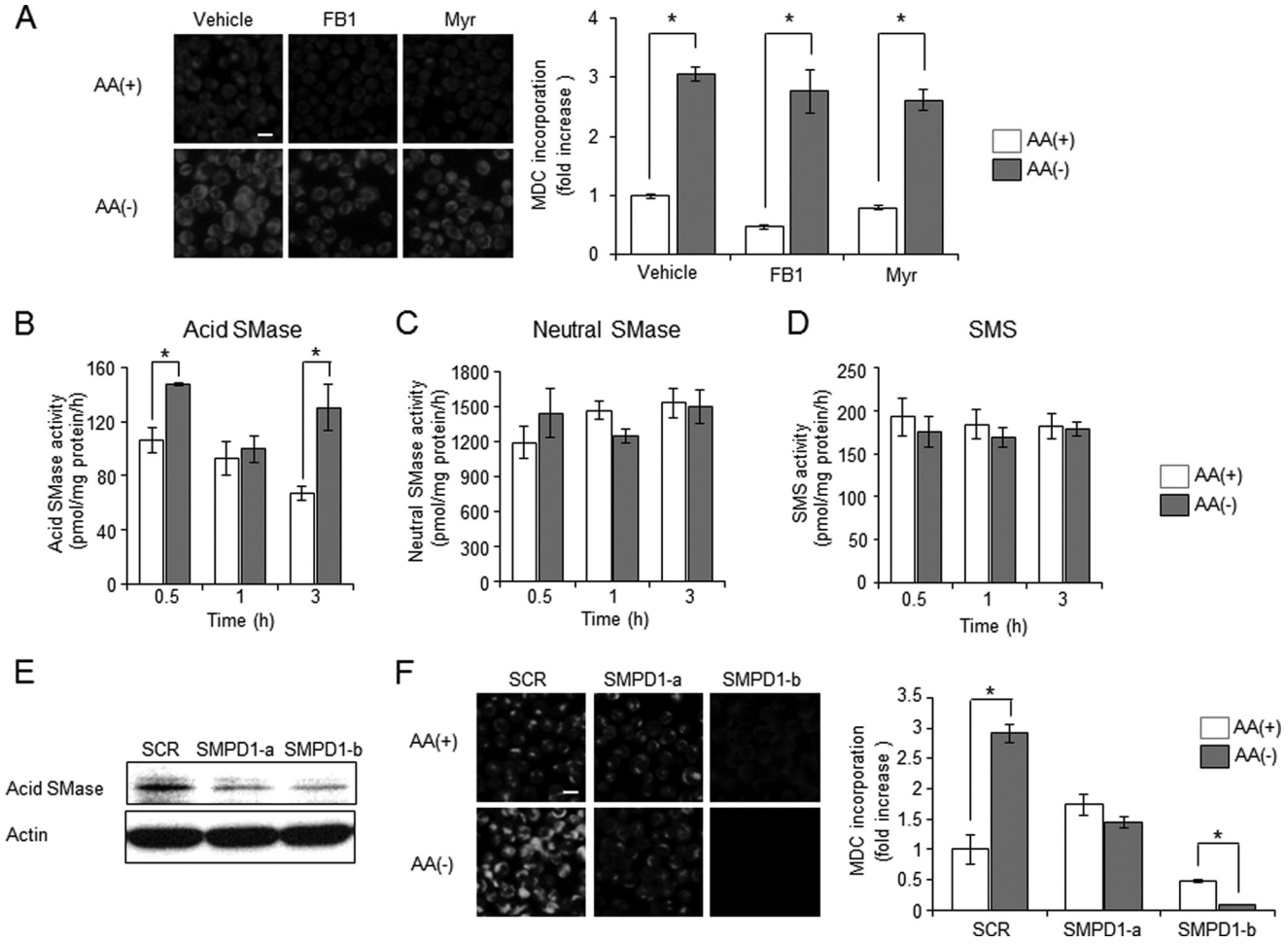

FIGURE 2. **Involvement of acid sphingomyelinase (SMase) in autophagy-mediated generation of ceramide.** *A*, HL-60 cells were cultured in AA(−) or AA(+) for 1 h after pre-treatment with 100 μM fumonisin B1 (*FB1*) or 100 nM myriosin (*Myr*) for 1 h. Autophagy was measured by MDC incorporation. *B–D*, cells were cultured in AA(−) or AA(+) for the indicated times, and then acid SMase (*B*), neutral SMase (*C*), and SMS (*D*) activities were measured using C_6-NBD-sphingomyelin and C_6-NBD-ceramide as the substrates as described under "Experimental Procedures." Values are the mean ± S.D. from three independent experiments. *, $p < 0.005$. *E* and *F*, HL-60 cells were transfected with 40 nM of two species of siRNAs for acid sphingomyelinase (*SMPD1-a* and *SMPD1-b*) and scrambled sequence siRNA using MultiFectam. Efficacy of siRNAs was checked by immunoblotting (*E*). Seventy-two hours after transfection, cells were incubated in AA(+) medium or AA(−) medium for 1 h. MDC incorporation was examined by fluorescence microscopy, and the density of MDC was calculated from at least 200 cells (*F*). Values are the mean ± S.D. from three independent experiments. *Scale bar*, 10 μM. *, $p < 0.005$.

These results indicate that AA(−) facilitates the formation of ceramide, which stimulates autophagy induction in HL-60 cells.

Acid SMase Is Involved in Autophagy Induction—Ceramide is synthesized by three enzymatic pathways: (i) *de novo* pathway, (ii) the sphingomyelin cycle consisting of SMase and SMS, and (iii) the salvage pathway. In previous studies, ceramide synthases, which are involved in *de novo* and salvage ceramide synthesis, have been implicated in the formation of autophagy-inducing ceramides (12, 13, 42). To elucidate the involvement of *de novo* and salvage pathways in autophagy, the effects of ceramide synthase inhibitor fumonisin B1 or ceramide *de novo* synthesis inhibitor myriocin on autophagy induction by AA(−) were tested in HL-60 cells. Neither treatment of HL-60 cells with fumonisin B1 nor myriocin affected the autophagy (Fig. 2*A*). Next to investigate the involvement of the sphingomyelin cycle, we determined enzyme activities such as SMase or SMS after AA(−) treatment. As shown Fig. 2, *B* and *C*, AA(−) treatment significantly activated acid SMase but not neutral SMase after 30 min and 3 h. On the other hand, SMS activity did not change in the AA(−) condition (Fig. 2*D*). To investigate whether acid SMase-dependent formation of ceramide contributes to AA(−)-induced autophagy, the effects of acid SMase knock-down were tested (Fig. 2*E*). As compared with scrambled sequence-treated cells, acid SMase knock-down significantly suppressed autophagy induction (Fig. 2*F*). These data suggest that acid SMase plays a role in AA(−)-induced ceramide production and autophagy.

S1P Treatment Counteracts Autophagy Induction by AA(−) or Ceramide—S1P is a potent proliferative lipid, and its effects are believed to result from its engagement with G-protein-coupled S1P receptors that generate mitogenic signaling. S1P signals protect cells from ceramide-dependent cell death signals (29), and that sphingolipid rheostat has been proposed to determine reciprocal cell fate. As ceramide was implicated in inducing autophagy and its associated cell death (13), we at first elucidated the effects of S1P on ceramide-dependent induction of autophagy. Treatment of HL-60 cells with S1P inhibited the formation of LC3 puncta and the generation of LC3-II induced by AA(−) (Fig. 3, *A* and *B*). Similarly, S1P treatment signifi-

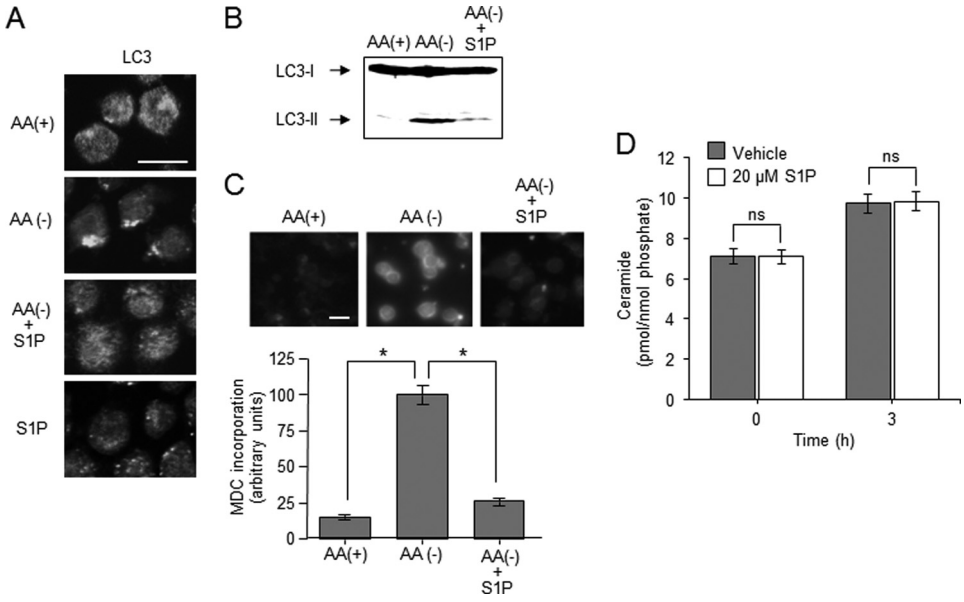

FIGURE 3. **Effects of S1P on AA(−)-induced autophagy.** *A*, HL-60 cells were incubated in AA(−) medium with 20 μM S1P for 1 h. Autophagosome formation was detected by immunostaining of LC-3. *Scale bar*, 10 μm. *B,* cells were incubated in AA(+) medium or AA(−) medium with or without 20 μM S1P for 1 h. LC3 protein was detected by Western blot analysis. *C,* after treatment with AA(+) or AA(−) together with or without S1P for 1 h, the cells were further incubated with 50 μM MDC for 10 min and immediately analyzed by fluorescence microscopy. The density of MDC was assessed using MacSCOPE. *Scale bar*, 10 μm. *D,* cells were incubated with AA(−) medium for the indicated times in the absence or presence of 20 μM S1P, and then the lipids were extracted. Ceramide content was measured using the diacylglycerol kinase method. Values are the mean ± S.D. from three independent experiments. *, $p < 0.005$; *ns*, no significance.

cantly attenuated AA(−)-induced incorporation of MDC in autophagosomes from 100 ± 6.5 to 25 ± 2.7 arbitrary units (Fig. 3*C*). On the other hand, treatment with S1P alone failed to form LC3 puncta in HL-60 cells (Fig. 3*A*). Next, we assessed whether S1P treatment affected AA(−)-induced formation of ceramide. As shown in Fig. 3*D*, S1P treatment had no effect on ceramide. These results suggest that S1P attenuates induction of autophagy by AA(−) without affecting ceramide formation in HL-60 cells.

In addition, we determined the effects of S1P on C_2-ceramide-induced autophagy. Immunocytochemistry of LC3 showed that S1P treatment inhibited the formation of LC3 puncta induced by C_2-ceramide (Fig. 4*A*). Similar to LC3 results, C_2-ceramide-induced incorporation of MDC was also significantly decreased by simultaneous treatment with 10 μM S1P from 45 ± 3.9 to 21 ± 2.7 arbitrary units (Fig. 4*B*). Even 20 μM S1P treatment also had inhibitory effects on autophagy induction. These data suggest that S1P offsets ceramide-mediated induction of autophagy.

S1P Treatment Activates the mTOR Pathway to Counteract Ceramide-mediated Induction of Autophagy—mTOR is conserved as a key molecule for cell responses to extracellular amino acids and growth factors in eukaryotic evolution (43, 44). In an amino acid-rich environment, mTOR is phosphorylated and activated, thereby suppressing autophagy induction. Amino acid withdrawal or ceramide treatment have been reported to inactivate mTOR signaling to promote autophagy, thereby raising possibilities that S1P is inhibiting autophagy by activating mTOR signaling. At first, we examined the effects of S1P on mTOR activation. AA(−) treatment decreased the levels of phosphorylated/activated mTOR at Ser-2448, and simultaneous treatment with S1P restored mTOR phosphorylation (Fig. 5*A*). In addition, we determined the kinase activity of mTOR in S1P-treated cells. An *in vitro* kinase assay using 4E-BP1 as a substrate revealed that S1P treatment significantly increased mTOR activity in a time- and dose-dependent manner (Fig. 5*B*). Consistently, S1P treatment potently promoted the phosphorylation of mTOR downstream targets such as p70 S6K and 4E-BP1 (β/γ forms) (Fig. 5*E*). These data suggest that S1P signaling targets the mTOR pathway. To further confirm this, we tested the effect of rapamycin on S1P-induced mTOR activation and autophagy inhibition. Rapamycin directly inhibits mTOR and shuts down its signaling pathway, inducing autophagy (45). As shown in Fig. 5, *C* and *D*, S1P treatment failed to counteract LC3-II formation and autophagy induction by rapamycin. This rapamycin treatment also blocked S1P-mediated phosphorylation of p70 S6K and 4E-BP1 (Fig. 5*E*). These results strongly suggest that S1P potentiates mTOR signaling and consequently counteracts autophagy induction by amino acid deprivation.

S1P-$S1P_3$ Receptor Signaling Offsets Autophagy—S1P binds to its cell surface receptors or intracellular target proteins, thereby generating biological responses. Therefore, we investigated how S1P affects mTOR-controlled autophagy. HL-60 cells have been reported to predominantly express $S1P_3$ (46). To confirm the gene expression profile of S1P receptors, Q-RT-PCR was performed. $S1P_3$ was predominantly expressed in HL-60 cells (Fig. 6*A*), confirming previous reports (47). To address whether $S1P_3$ plays a key role in autophagy inhibition by S1P, we examined the effect of the $S1P_3$ antagonist CAY10444 on S1P-mediated counteraction of autophagy. Antagonism of $S1P_3$ receptor by CAY10444 offset an inhibitory effect of S1P on LC3-II formation by AA(−) (Fig. 6*B*), suggesting a novel role of $S1P_3$ in suppressing autophagy in HL-60 cells. To further corroborate the importance of $S1P_3$, we employed $S1P_3$-overexpressing CHO cells (CHO/$S1P_3$) (32). To examine

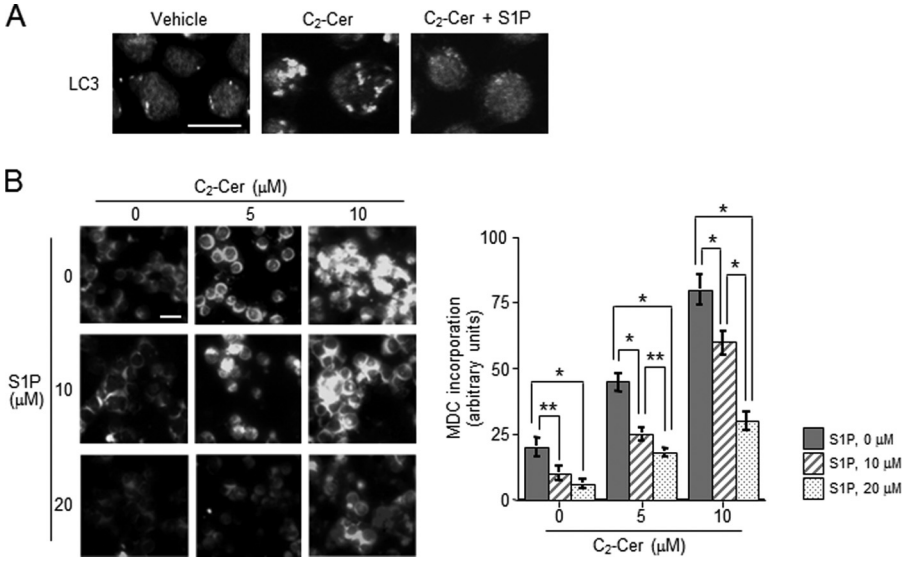

FIGURE 4. **Effects of S1P on ceramide-induced autophagy.** *A,* HL-60 cells were treated with 10 μM C_2-ceramide (C_2-Cer) for 1 h in AA(+) medium. Autophagosome formation was detected with LC-3 staining. *Scale bar*, 10 μm. *B,* cells were treated with the combination of C_2-Cer and S1P at various concentration for 30 min in AA(+) medium. After treatment with C_2-Cer and S1P at the indicated concentrations, autophagy was assessed by MDC incorporation under fluorescence microscopy and measured using MacSCOPE. Values are the mean ± S.D. from three independent experiments. *, $p < 0.005$; **, $p < 0.05$.

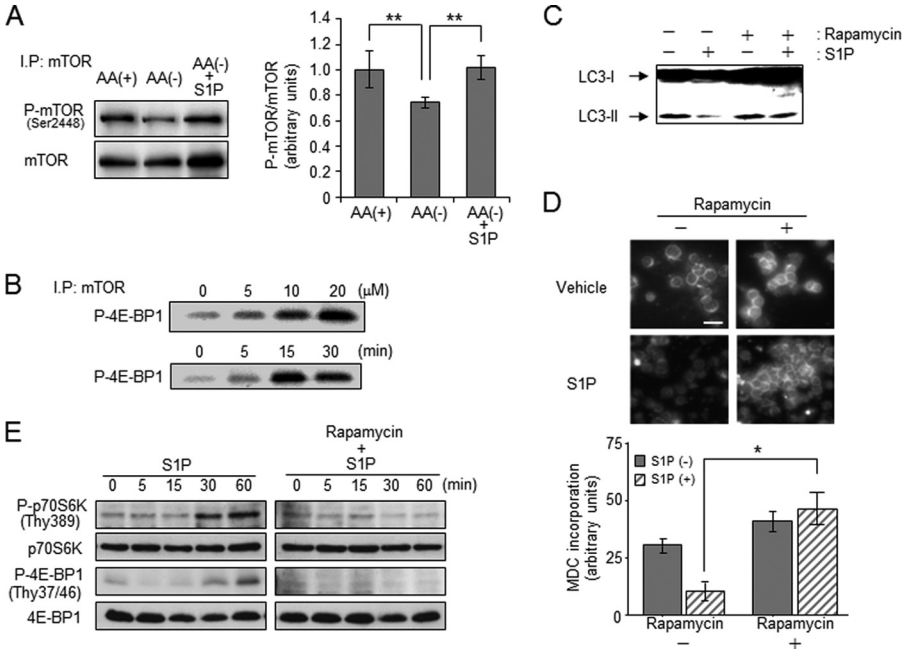

FIGURE 5. **Effect of S1P on the activation of mTOR pathway- and rapamycin-induced autophagy.** *A,* HL-60 cells were incubated in AA(+) or AA(−) with or without 20 μM S1P for 30 min. Western blot analysis was performed using the anti-phospho-mTOR (Ser-2448) antibody or anti-mTOR antibody after immunoprecipitation using the anti-mTOR antibody. Phospho-mTOR/mTOR levels were quantified with ImageJ 1.43. Values are the mean ± S.D. from three independent experiments. **, $p < 0.05$. *B*, cells were treated with various concentrations of S1P for 30 min (*upper panel*) or with 20 μM S1P for the indicated times (*lower panel*). *In vitro* kinase activity in immunoprecipitated mTOR was measured. *C* and *D,* cells were incubated with AA(−) medium for 1 h in the presence or absence of 20 μM S1P with or without pretreatment with 50 nM rapamycin for 24 h. LC3 protein was determined by Western blot analysis (*C*), and autophagy was detected by MDC incorporation and measured using MacSCOPE (*D*). *Scale bar*, 10 μm. Values are the mean ± S.D. from three independent experiments. *, $p < 0.005$. *E*, cells were incubated in AA(−) medium for the indicated times in the presence of 20 μM S1P with or without 50 nM rapamycin pretreatment for 24 h. Western blot analysis was performed using the anti-phospho-p70 S6 kinase (*P-p70 S6K*), anti-p70 S6K, anti-phospho-4E-BP1, and anti-4E-BP1 antibodies. Results are representative of three independent experiments.

$S1P_3$ involvement in offsetting autophagy, we employed the $S1P_3$ overexpression system with CHO cells. AA(−) treatment decreased mTOR phosphorylation in CHO and $S1P_3$-overexpressing CHO cells (CHO/$S1P_3$). Subsequent S1P treatment increased phosphorylation of mTOR in a dose-dependent manner, which was specific to CHO/$S1P_3$ cells. Its EC_{50} was ~2.93 μM. Akt and ERK are known as downstream factors of the S1P-S1P receptor (28), those kinases were also activated by S1P treatment in CHO/$S1P_3$ but not CHO cells (Fig. 7*A*). S1P treatment also increased phosphorylation/activation of mTOR downstream proteins such as p70 S6K or 4E-BP1 in CHO/$S1P_3$ cells (Fig. 7, *A* and *B*). Consistent with HL60 cells, S1P treatment is suggested to stimulate the mTOR pathway through the $S1P_3$ receptor. In CHO cells, C_2-ceramide treatment also pro-

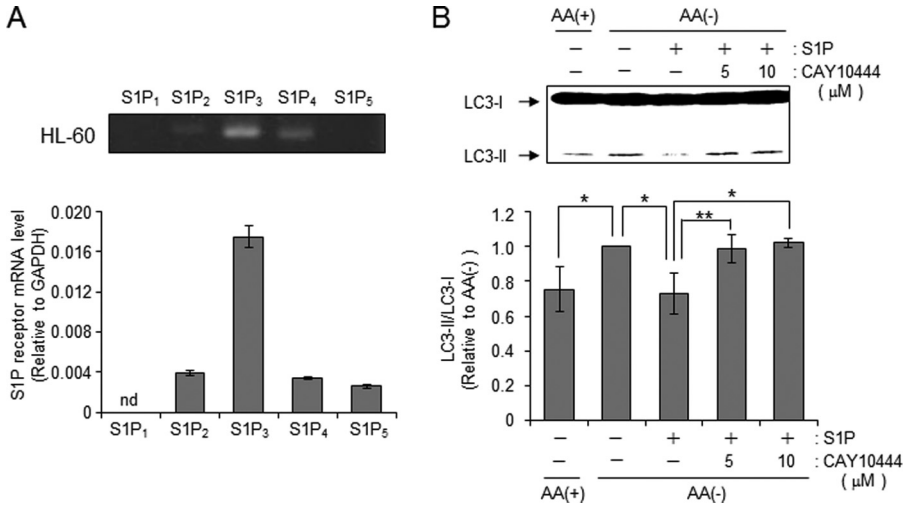

FIGURE 6. **$S1P_3$ receptor is essential for S1P-mediated counteraction of autophagy.** *A*, expression of S1P receptors ($S1P_{1-5}$) was detected by RT-PCR (*upper panel*) and real-time PCR (*under graph*) in HL-60 cells. Total RNA was extracted from cells and converted to cDNA. The real-time PCR was performed for both the target gene and GAPDH. Expression was calculated after normalizing against GAPDH in each sample and is presented as relative mRNA expression. *B*, cells were incubated in either AA(+) or AA(−), either alone or supplemented with 20 μM S1P in the presence or absence of CAY10444 for 30 min. LC3 protein was detected by immunoblotting, and LC3-II/LC3-I levels were quantified with ImageJ 1.43. Values are the mean ± S.D. from three independent experiments. *, $p < 0.005$. **, $p < 0.05$.

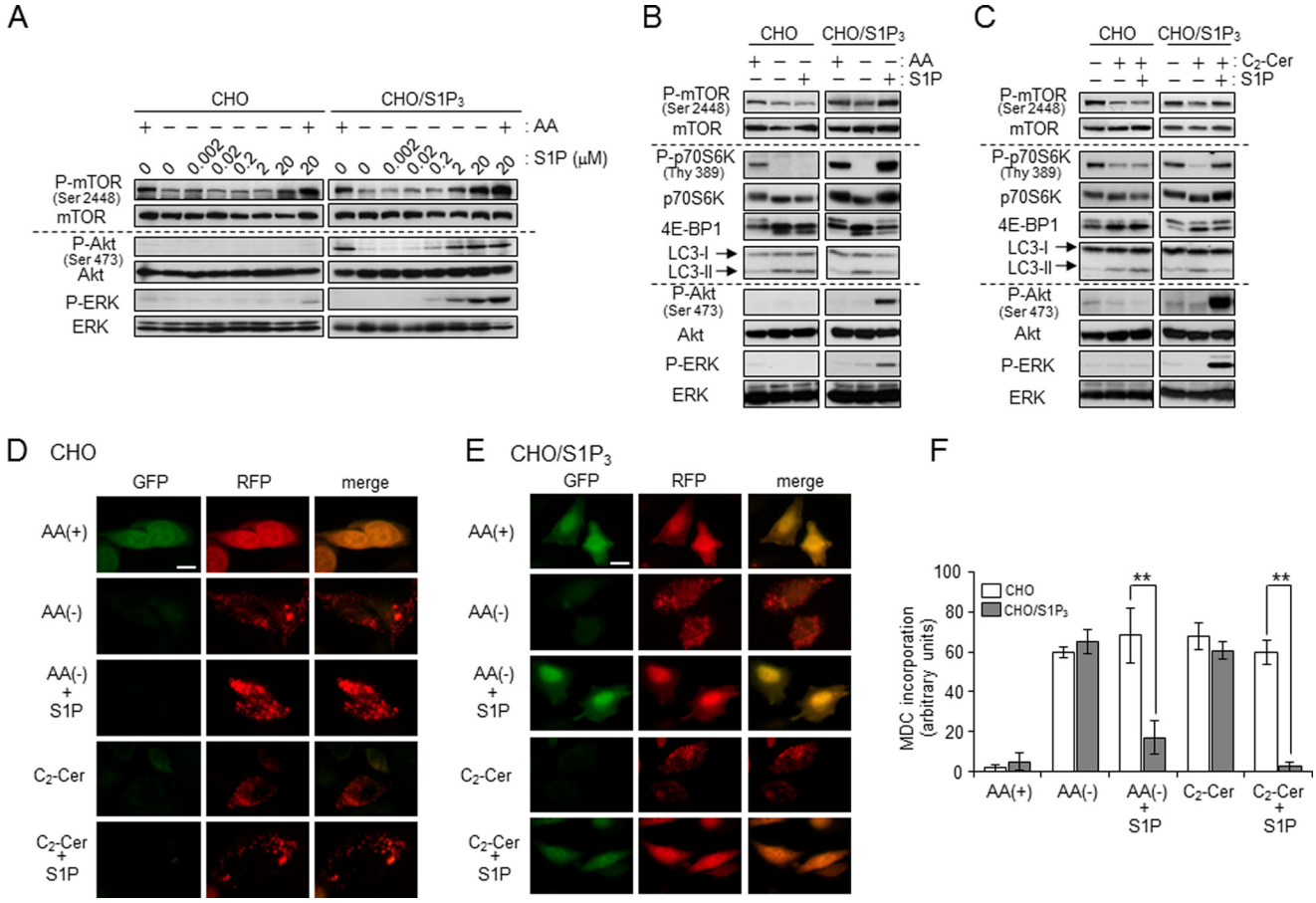

FIGURE 7. **S1P-$S1P_3$ receptor signaling accelerates mTOR pathway interference with ceramide-dependent autophagy.** *A*, CHO and CHO/$S1P_3$ cells were cultured in AA(−) or serum-free medium (AA(+)) containing the indicated concentrations of S1P for 30 min. Each protein was detected by Western blot analysis. *B* and *C*, CHO and CHO/$S1P_3$ cells were cultured in AA(−) with or without 10 μM S1P for 30 min (*B*) or treated with 50 μM C_2-ceramide (*C_2-Cer*) in the presence or absence of 10 μM S1P for 30 min (*C*). The indicated proteins were detected by immunoblotting. *D* and *E*, CHO (*D*) and CHO/$S1P_3$ (*E*) cells were transfected with RFP-GFP-LC3 using the TransIT-LT1 (Mirus). After 36 h, cells were cultured in serum-free media for 3 h, and treated with each condition for 60 min. Images were obtained by fluorescent microscopy. *Scale bars*, 10 μm. *F*, CHO cell lines were cultured in AA(−) or serum-free medium (AA(+)) containing 50 μM C_2-Cer with or without 10 μM S1P for 30 min. Then, MDC incorporation was examined by fluorescence microscopy, and the density of MDC was calculated. Images were obtained by fluorescent microscopy, and cells having at least five dots were counted as autophagic cells. Values are the mean ± S.D. from three independent experiments. **, $p < 0.05$.

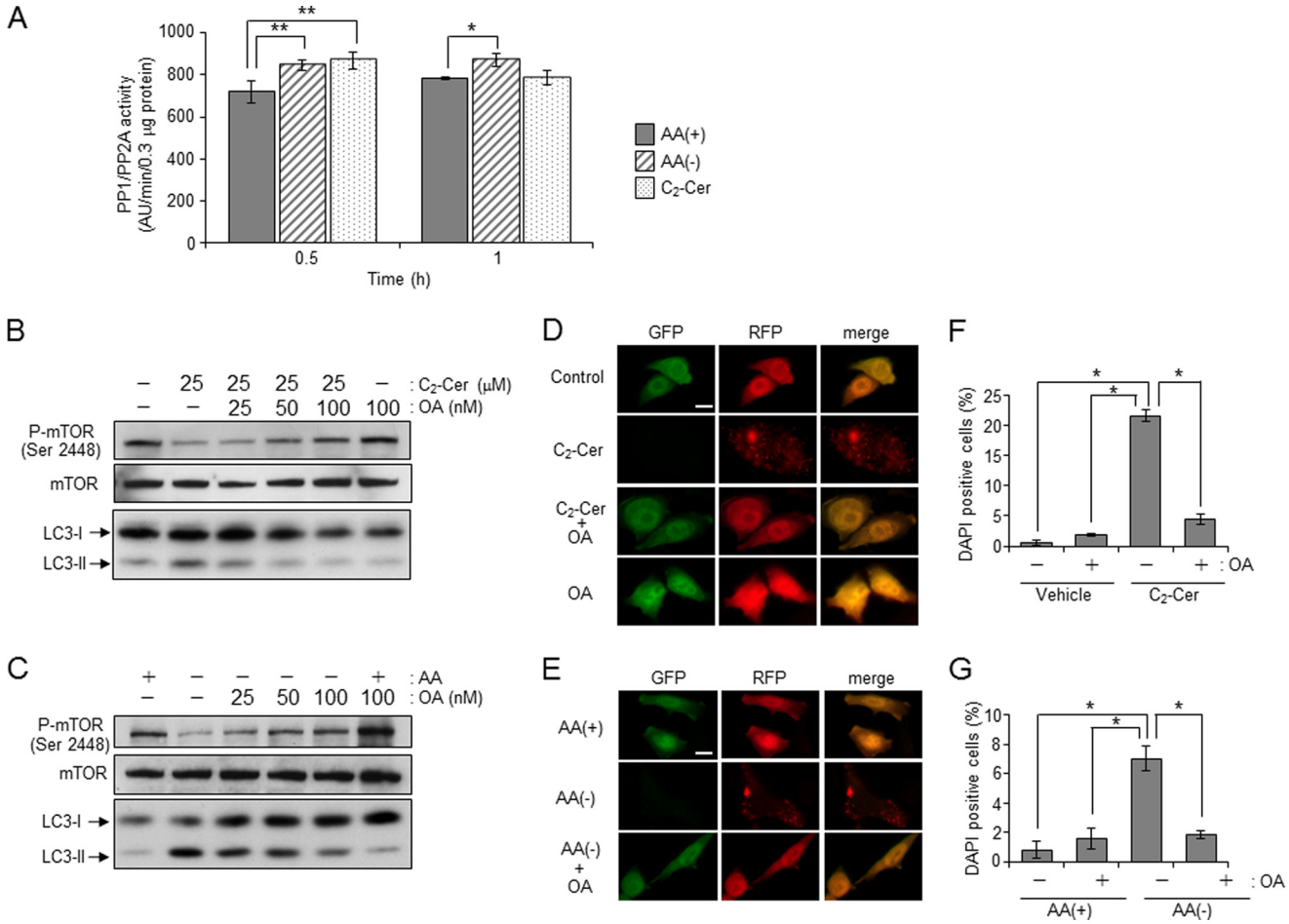

FIGURE 8. **Involvement of CAPPs on mTOR dephosphorylation and ceramide-dependent autophagy.** *A,* CHO/S1P$_3$ cells were treated with AA(+), AA(−), or 10 μM C_2-ceramide (*C_2-Cer*) for 30 or 60 min, and then cells were harvested. PP1/PP2A serine/threonine protein phosphatase activity was determined as described under "Experimental Procedures." The specific activity expressed as arbitrary unit/min/0.3 μg of protein. *B* and *C,* CHO/S1P$_3$ cells were incubated with or without OA in serum-free media for 3 h. Cells were treated with C_2-Cer (*B*) or AA(−) (*C*) for 1 h. Phosphor-mTOR and mTOR was detected by Western blot analysis. *D* and *E,* RFP-GFP-LC3 was transfected in CHO/S1P$_3$ cells. After 36 h, cells were treated with C_2-Cer (*D*) or AA(−) (*E*) in the presence or absence of 100 nM OA. Images were obtained by fluorescent microscopy. *Scale bars*, 10 μm. *F* and *G,* cells were treated with 50 μM C_2-Cer (*F*) or AA(−) (*C*) with or without 100 nM OA for 12 h. Cell death was assessed by DAPI staining and at least 100 cells were counted. Values are the mean ± S.D. from three independent experiments. *, $p < 0.005$. **, $p < 0.05$.

moted the dephosphorylation of mTOR and inactivated the mTOR pathway in the absence or presence of S1P, whereas CHO/S1P$_3$ cells stimulated with S1P showed increased phosphorylation in mTOR even in the presence of ceramide (Fig. 7*C*). These results indicate that extracellular S1P activates S1P$_3$ receptors and in turn counteracts the effects of ceramide. Consistent with mTOR phosphorylation, the increase in LC3-II formation by AA(−) or C_2-ceramide was suppressed by treatment with S1P in CHO/S1P$_3$ cells, but not CHO cells (Fig. 7, *B* and *C*).

In addition, we examined the effects of S1P-S1P$_3$ receptors on autophagosome formation. tfLC3 (36) has green and red fluorescence in steady-state conditions but loses the green fluorescence in acidic compartments such as autophagosome lysosomes. As shown in Fig. 7, *D* and *E*, AA(−) and C_2-ceramide treatment induced the disappearance of green fluorescence and puncta of red fluorescence in both CHO and CHO/S1P$_3$ cells. Selective to CHO/S1P$_3$ cells, S1P treatment inhibited AA(−)- and C_2-ceramide-induced formation of LC3 pancta. Similar to LC3 puncta formation, inhibition of autophagy by S1P treatment was confirmed to occur in only CHO/S1P$_3$ cells with the MDC incorporation assay (Fig. 7*F*). These data suggest that the S1P-S1P$_3$ signal activates the mTOR pathway, counteracting autophagy induction by the AA(−)-ceramide signal.

Involvement of CAPPs in mTOR Dephosphorylation/Inactivation—The above data show that ceramide induces autophagy by promoting dephosphorylation/inactivation of mTOR signaling. Ceramide has been shown to activate serine/threonine protein phosphatase containing PP1 and PP2A, which are called CAPPs (47, 48). Thus we determined the activity of PP1/PP2A in AA(−) or C_2-ceramide-treated cells. Both treatments with AA(−) and C_2-ceramide increased PP1/PP2A activity as compared with AA(+) treatment after 30 min (Fig. 8*A*). To clarify the involvement of PP1/PP2A in ceramide-mediated dephosphorylation of mTOR, we employed okadaic acid (49), which is a specific inhibitor for PP2A and PP1. As shown in Fig. 8*B*, C_2-ceramide treatment clearly facilitated dephosphorylation of mTOR in CHO/S1P$_3$ cells, and okadaic acid treatment blocked its dephosphorylation in a dose-dependent manner. Furthermore, okadaic acid treatment also inhibited LC3 puncta formation (Fig. 8*D*). Similarly, okadaic acid treatment also suppressed both mTOR dephosphorylation and LC3 puncta formation induced by AA(−) (Fig. 8, *C* and *E*). These

results indicate that okadaic acid-sensitive CAPPs are involved in dephosphorylation of mTOR induced by AA(−) and C_2-ceramide followed by autophagy induction. Furthermore, okadaic acid treatment also suppressed cell death induced by both AA(−) and C_2-ceramide (Fig. 8, *F* and *G*), implicating the involvement of a ceramide-dependent cellular signal in cell death concomitant with autophagy.

S1P Protects Autophagy-associated Cell Death as a Survival Lipid—In mammalian cells, autophagy exerts cytoprotective effects against nutrient deprivation, whereas prolonged autophagy destroys the cytosol and organelles, inducing cell death, namely autophagy-associated cell death. To investigate whether autophagy has a role as cell death or cell survival in HL-60, we employed 3-MA, which is known as an autophagy inhibitor targeting class III PI 3-kinase. As shown Fig. 9*A*, 3-MA treatment was confirmed to inhibit LC3-II formation induced by AA(−). Next, we monitored cell death by DAPI staining in those conditions. Approximately 50% of cells displayed significant chromatin condensation after 2 h of AA(−) treatment (Fig. 9*B*). 3-MA treatment slightly increased cell death in control cells, whereas its treatment significantly suppressed AA(−)-induced cell death. Those data suggested that autophagy triggers cell death induction. Moreover, we investigated whether S1P protects autophagy-associated cell death. S1P co-treatment decreased the number of DAPI-positive cells in AA(−)-treated HL-60 cells (Fig. 10*A*). Treatment with C_2-ceramide also increased cell death, whereas S1P treatment inhibited C_2-ceramide-induced cell death in a dose-dependent manner. Similar to HL-60 cells, S1P treatment significantly blocked autophagy-associated cell death induced by both AA(−) and C_2-ceramide in CHO/$S1P_3$ cells (Fig. 10, *C* and *D*, *gray column*). However, S1P could not prevent autophagy-associated cell death in CHO cells (Fig. 10, *C* and *D*, *white column*). Those results also indicate specific involvement of the S1P-$S1P_3$ pathway in the offset of autophagy-associated cell death activity.

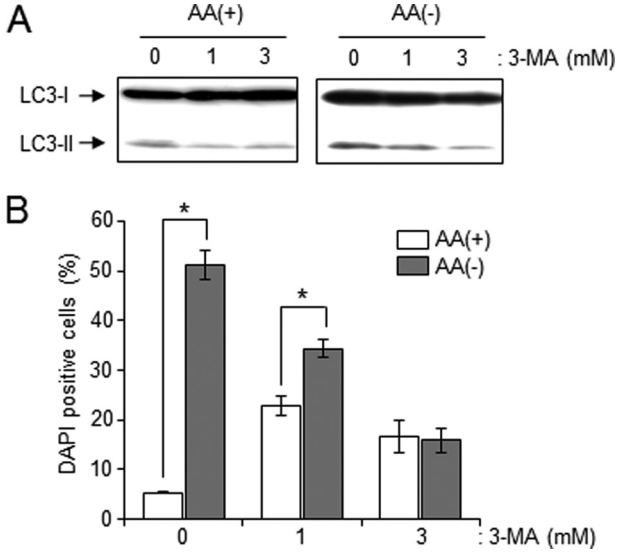

FIGURE 9. **Inhibition of AA(−)-mediated autophagy leads to escape from autophagy-associated cell death.** *A*, HL-60 cells were cultured in AA(−) or AA(+) with or without 3-MA (1 and 3 mM) for 30 min. LC3 protein was detected by Western blot analysis. The results are representative of three independent experiments. *B,* after a 2-h treatment with 3-MA in AA(−) or AA(+), cell death was assessed by DAPI staining and at least 100 cells were counted. Values are the mean ± S.D. from three independent experiments. *, $p < 0.005$.

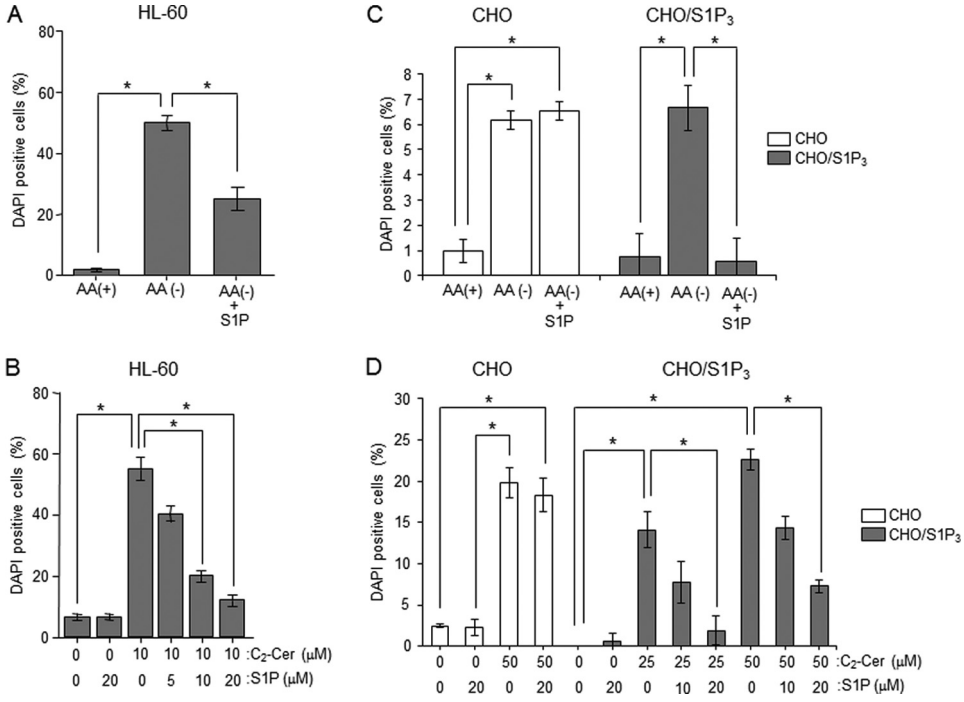

FIGURE 10. **Effects of S1P on autophagy-associated cell death following ceramide treatment.** *A,* HL-60 cells were incubated in AA(+) or AA(−) with or without 20 μM S1P for 2 h. *B*, cells were incubated with the indicated concentrations of S1P (0, 5, 10, and 20 μM) and 10 μM C_2-ceramide (*C_2-Cer*) for 24 h in AA(+) medium. *C,* CHO (*white column*) and CHO/$S1P_3$ (*gray column*) cells were incubated in AA(+) or AA(−) with or without 20 μM S1P for 12 h. *D*, cells were incubated with various combinations of S1P (0, 10, and 20 μM) and C_2-Cer (0, 25, and 50 μM) for 6 h. Cell death was assessed by DAPI staining. Values are the mean ± S.D. from three independent experiments. *, $p < 0.005$; **, $p < 0.05$.

DISCUSSION

In the present study, we uncovered the inhibitory effects of S1P on ceramide-mediated induction of autophagy. AA(−) stimulates acid SMase to generate ceramide that promotes the formation of autophagosomes, followed by autophagy-associated cell death. The regulation of mTOR by ceramide plays a key role in these biological responses, and S1P-$S1P_3$ signals counteract autophagy induction by activating the mTOR pathway. These findings demonstrate for the first time that cellular signaling arising from distinct actions of S1P and ceramide commonly target the mTOR pathway, leading to reciprocal regulation of autophagy and its associated cell death. Thus, the rheostat between sphingolipids is proposed to play an important role in autophagy regulation.

First, we showed that AA(−) induced an increase in ceramide. In apoptotic cell death, ceramide was mainly generated through activation of the *de novo* pathway or inhibition of the "sphingomyelin cycle" (50–53). Some reports showed that autophagy accompanied ceramide formation through ceramide synthase, which mediates both *de novo* and salvage pathway (12, 13, 42). However, inhibition of ceramide synthases by fumonisin B had no effects on AA(−)-mediated autophagy in our system (Fig. 2). On the other hand, we found an increase of acid SMase activity with AA(−) treatment, and acid SMase knock-down suppressed autophagy induction (Fig. 2). These results suggested the implication of acid SMase in AA(−) stimulation of ceramide and autophagy induction. However, the mechanism by which AA(−) treatment activates acid SMase activation remains unclear.

Ceramide has been reported to inactivate the mTOR pathway or dissociate the beclin1-Bcl-2 complex, leading to autophagy (12, 15, 24). We have shown that ceramide elevation promotes mTOR dephosphorylation at Ser-2448 (Fig. 9). Okadaic acid-sensitive protein phosphatases such as CAPPs have been reported to interfere with the signal of mTOR whose upstream kinase is Akt. Ceramide is also known to promote the dephosphorylation and inactivation of Akt (54, 55). Although we are yet to identify CAPP substrates, the ceramide-CAPP pathway is suggested to have an inhibitory effect on the mTOR pathway, which in turn induces autophagy. Our studies demonstrate, for the first time, an involvement of CAPPs in autophagy induction, and we propose that inactivation of the mTOR pathway by ceramide-CAPPs plays a key role in the induction of autophagy.

S1P has been emerging as a cell proliferative lipid messenger. Intrinsic S1P-induced autophagy protects cells from cell death with apoptotic hallmarks during nutrient starvation (24). In contrast, we showed that extrinsic S1P inhibited ceramide-dependent induction of autophagy by engaging the $S1P_3$ receptors (Fig. 7). These reciprocal results raise the possibility that intrinsic regulation of autophagy by S1P is distinct from its extrinsic function. Interestingly, S1P/$S1P_3$-mediated inhibition of autophagy led to the protection of cells from autophagy-associated cell death (Fig. 10). S1P is suggested to have reciprocal effects on autophagy induction, and even distinctly compartmentalized S1P exerted cell survival effects.

Consistent with a previous report (46), we confirmed that HL-60 cells predominantly expressed $S1P_3$ (Fig. 6). Banno *et al.* (56) demonstrated that the S1P-$S1P_3$ receptor axis activated the PI 3-kinase-Akt pathway and promoted proliferation. Proliferative stimulation with growth factors activated Akt, which in turn phosphorylated mTOR (57). Similarly S1P-$S1P_3$ signaling had stimulatory effects on the phosphorylation of Akt at Ser-473 and mTOR at 2448, and its downstream signals such as ERK1/2, p70 S6 kinase, and 4E-BP1 and inhibited ceramide-dependent autophagy (Fig. 7). mTOR forms two functional complexes, the rapamycin-sensitive mTOR complex 1 (mTORC1) and rapamycin-insensitive mTORC2 (58, 59). It was recently reported that the PI 3-kinase-PDK1-mTORC1 and mTORC2 pathways independently regulate the phosphorylation of Akt at Ser-473 and Thr-308 (60). The activation of Akt at Ser-473 was negatively involved in FOXO3a translocation to the nucleus, leading to apoptotic cell death resistance (54, 60). These data may suggest that extrinsic S1P activates Akt downstream of mTORC2, but the precise involvement of mTORC2 as compared with mTORC1 in S1P-inhibited autophagy remains to be elusive.

S1P receptors have nanomolar binding affinities for S1P (19, 21, 61, 62). Our results showed that treatments of $S1P_3$ overexpressing CHO cells with S1P (0.2–10 μM) activated mTOR, Akt, and ERK (Fig. 7), and we have determined the EC_{50} from Western blot results (Fig. 7*A*). The EC_{50} values of S1P for the phosphorylation of mTOR, Akt, and ERK are 2.93, 2.59, and 2.4 μM, respectively. For the considered K_d values (0.23 nM) between S1P and $S1P_3$ receptor (61), those EC_{50} values appear to be high. Indeed, some reports also showed the high values for S1P EC_{50}. Okajima *et al.* (63) showed that S1P treatment increases intracellular Ca^{2+} in HL-60 cells, and its S1P EC_{50} was 1–2 μM. Moreover, S1P EC_{50} value of A549 cells for prostaglandin E_2 production was also shown to be ~0.85 μM (64). What decreases the susceptibility to S1P remains unknown.

Recently, Liu *et al.* reported that $S1P_1$ signaling activates the Akt-mTOR pathway to impede the development and function of regulatory T cells (65), but HL-60 cells had no detectable expression of $S1P_1$ receptors (Fig. 6). In $S1P_2$ or $S1P_4$ expressing CHO cells, S1P treatment failed to counteract AA(−)- or ceramide-induced autophagy, although S1P was capable of activating ERK2 through both $S1P_2$ and $S1P_4$, whose mRNAs were faintly detectable in HL-60 cells (Fig. 6 and supplemental Fig. S1). On the other hand, $S1P_5$ receptor mRNA was detectable in Q-RT-PCR (Fig. 6). Chang *et al.* showed that $S1P_5$ is involved in autophagy induction at the long time serum starvation condition in PC3 cells (66). However, S1P treatment had no effects on autophagy induced by AA(−) in $S1P_5$ overexpressing CHO cells (supplemental Fig. S2). Therefore, these results strongly indicate that inhibitory effects of S1P on ceramide-induced autophagy and its associated cell death in HL-60 cells were attributed to $S1P_3$ signaling. Furthermore, using CHO/$S1P_3$ cells, we also demonstrated that S1P-$S1P_3$ signaling facilitates the activation of the mTOR pathway, which lead to autophagy suppression. In conclusion, ceramide-CAPPs and the S1P-$S1P_3$ pathway reciprocally regulate autophagy by targeting the mTOR pathway. We proposed that the "sphingolipid rheostat" by ceramide and S1P serves as a novel biological system for

controlling mTOR-regulated autophagy and its associated cell death.

REFERENCES

1. Ogretmen, B., and Hannun, Y. A. (2004) Biologically active sphingolipids in cancer pathogenesis and treatment. *Nat. Rev. Cancer* **4,** 604–616
2. Zheng, W., Kollmeyer, J., Symolon, H., Momin, A., Munter, E., Wang, E., Kelly, S., Allegood, J. C., Liu, Y., Peng, Q., Ramaraju, H., Sullards, M. C., Cabot, M., and Merrill, A. H., Jr. (2006) Ceramides and other bioactive sphingolipid backbones in health and disease. Lipidomic analysis, metabolism, and roles in membrane structure, dynamics, signaling and autophagy. *Biochim. Biophys. Acta* **1758,** 1864–1884
3. Spiegel, S., and Milstien, S. (2003) Sphingosine-1-phosphate. An enigmatic signalling lipid. *Nat. Rev. Mol. Cell Biol.* **4,** 397–407
4. Hannun, Y. A. (1996) Functions of ceramide in coordinating cellular responses to stress. *Science* **274,** 1855–1859
5. Kolesnick, R. N., and Krönke, M. (1998) Regulation of ceramide production and apoptosis. *Annu. Rev. Physiol.* **60,** 643–665
6. Kitatani, K., Idkowiak-Baldys, J., and Hannun, Y. A. (2008) The sphingolipid salvage pathway in ceramide metabolism and signaling. *Cell. Signal.* **20,** 1010–1018
7. Merrill, A. H., Jr., Schmelz, E. M., Dillehay, D. L., Spiegel, S., Shayman, J. A., Schroeder, J. J., Riley, R. T., Voss, K. A., and Wang, E. (1997) Sphingolipids: the enigmatic lipid class. Biochemistry, physiology, and pathophysiology. *Toxicol. Appl. Pharmacol.* **142,** 208–225
8. Hannun, Y. A., and Obeid, L. M. (2008) Principles of bioactive lipid signalling. Lessons from sphingolipids. *Nat. Rev. Mol. Cell Biol.* **9,** 139–150
9. Futerman, A. H., and Riezman, H. (2005) The ins and outs of sphingolipid synthesis. *Trends Cell Biol.* **15,** 312–318
10. Chalfant, C. E., Ogretmen, B., Galadari, S., Kroesen, B. J., Pettus, B. J., and Hannun, Y. A. (2001) FAS activation induces dephosphorylation of SR proteins. Dependence on the de novo generation of ceramide and activation of protein phosphatase 1. *J. Biol. Chem.* **276,** 44848–44855
11. Santana, P., Peña, L. A., Haimovitz-Friedman, A., Martin, S., Green, D., McLoughlin, M., Cordon-Cardo, C., Schuchman, E. H., Fuks, Z., and Kolesnick, R. (1996) Acid sphingomyelinase-deficient human lymphoblasts and mice are defective in radiation-induced apoptosis. *Cell* **86,** 189–199
12. Scarlatti, F., Bauvy, C., Ventruti, A., Sala, G., Cluzeaud, F., Vandewalle, A., Ghidoni, R., and Codogno, P. (2004) Ceramide-mediated macroautophagy involves inhibition of protein kinase B and up-regulation of beclin 1. *J. Biol. Chem.* **279,** 18384–18391
13. Salazar, M., Carracedo, A., Salanueva, I. J., Hernández-Tiedra, S., Lorente, M., Egia, A., Vázquez, P., Blázquez, C., Torres, S., García, S., Nowak, J., Fimia, G. M., Piacentini, M., Cecconi, F., Pandolfi, P. P., González-Feria, L., Iovanna, J. L., Guzmán, M., Boya, P., and Velasco, G. (2009) Cannabinoid action induces autophagy-mediated cell death through stimulation of ER stress in human glioma cells. *J. Clin. Invest.* **119,** 1359–1372
14. Park, M. A., Zhang, G., Martin, A. P., Hamed, H., Mitchell, C., Hylemon, P. B., Graf, M., Rahmani, M., Ryan, K., Liu, X., Spiegel, S., Norris, J., Fisher, P. B., Grant, S., and Dent, P. (2008) Vorinostat and sorafenib increase ER stress, autophagy and apoptosis via ceramide-dependent CD95 and PERK activation. *Cancer Biol. Ther.* **7,** 1648–1662
15. Pattingre, S., Bauvy, C., Carpentier, S., Levade, T., Levine, B., and Codogno, P. (2009) Role of JNK1-dependent Bcl-2 phosphorylation in ceramide-induced macroautophagy. *J. Biol. Chem.* **284,** 2719–2728
16. Spiegel, S., and Kolesnick, R. (2002) Sphingosine 1-phosphate as a therapeutic agent. *Leukemia* **16,** 1596–1602
17. An, S., Bleu, T., Huang, W., Hallmark, O. G., Coughlin, S. R., and Goetzl, E. J. (1997) Identification of cDNAs encoding two G protein-coupled receptors for lysosphingolipids. *FEBS Lett.* **417,** 279–282
18. Lee, M. J., Van Brocklyn, J. R., Thangada, S., Liu, C. H., Hand, A. R., Menzeleev, R., Spiegel, S., and Hla, T. (1998) Sphingosine-1-phosphate as a ligand for the G protein-coupled receptor EDG-1. *Science* **279,** 1552–1555
19. Van Brocklyn, J. R., Gräler, M. H., Bernhardt, G., Hobson, J. P., Lipp, M., and Spiegel, S. (2000) Sphingosine-1-phosphate is a ligand for the G protein-coupled receptor EDG-6. *Blood* **95,** 2624–2629
20. Yamazaki, Y., Kon, J., Sato, K., Tomura, H., Sato, M., Yoneya, T., Okazaki, H., Okajima, F., and Ohta, H. (2000) Edg-6 as a putative sphingosine 1-phosphate receptor coupling to Ca^{2+} signaling pathway. *Biochem. Biophys. Res. Commun.* **268,** 583–589
21. Im, D. S., Heise, C. E., Ancellin, N., O'Dowd, B. F., Shei, G. J., Heavens, R. P., Rigby, M. R., Hla, T., Mandala, S., McAllister, G., George, S. R., and Lynch, K. R. (2000) Characterization of a novel sphingosine 1-phosphate receptor, Edg-8. *J. Biol. Chem.* **275,** 14281–14286
22. Pyne, S., and Pyne, N. J. (2002) Sphingosine 1-phosphate signalling and termination at lipid phosphate receptors. *Biochim. Biophys. Acta* **1582,** 121–131
23. Hait, N. C., Allegood, J., Maceyka, M., Strub, G. M., Harikumar, K. B., Singh, S. K., Luo, C., Marmorstein, R., Kordula, T., Milstien, S., and Spiegel, S. (2009) Regulation of histone acetylation in the nucleus by sphingosine-1-phosphate. *Science* **325,** 1254–1257
24. Lavieu, G., Scarlatti, F., Sala, G., Carpentier, S., Levade, T., Ghidoni, R., Botti, J., and Codogno, P. (2006) Regulation of autophagy by sphingosine kinase 1 and its role in cell survival during nutrient starvation. *J. Biol. Chem.* **281,** 8518–8527
25. Lépine, S., Allegood, J. C., Park, M., Dent, P., Milstien, S., and Spiegel, S. (2011) Sphingosine-1-phosphate phosphohydrolase-1 regulates ER stress-induced autophagy. *Cell Death Differ.* **18,** 350–361
26. Potteck, H., Nieuwenhuis, B., Lüth, A., van der Giet, M., and Kleuser, B. (2010) Phosphorylation of the immunomodulator FTY720 inhibits programmed cell death of fibroblasts via the S1P3 receptor subtype and Bcl-2 activation. *Cell Physiol. Biochem.* **26,** 67–78
27. Maeurer, C., Holland, S., Pierre, S., Potstada, W., and Scholich, K. (2009) Sphingosine-1-phosphate induced mTOR-activation is mediated by the E3-ubiquitin ligase PAM. *Cell Signal* **21,** 293–300
28. Kluk, M. J., and Hla, T. (2001) Role of the sphingosine 1-phosphate receptor EDG-1 in vascular smooth muscle cell proliferation and migration. *Circ. Res.* **89,** 496–502
29. Bektas, M., Jolly, P. S., Müller, C., Eberle, J., Spiegel, S., and Geilen, C. C. (2005) Sphingosine kinase activity counteracts ceramide-mediated cell death in human melanoma cells. Role of Bcl-2 expression. *Oncogene* **24,** 178–187
30. Taha, T. A., Kitatani, K., El-Alwani, M., Bielawski, J., Hannun, Y. A., and Obeid, L. M. (2006) Loss of sphingosine kinase-1 activates the intrinsic pathway of programmed cell death. Modulation of sphingolipid levels and the induction of apoptosis. *FASEB J.* **20,** 482–484
31. Maceyka, M., Payne, S. G., Milstien, S., and Spiegel, S. (2002) Sphingosine kinase, sphingosine-1-phosphate, and apoptosis. *Biochim. Biophys. Acta* **1585,** 193–201
32. Kohno, T., and Igarashi, Y. (2003) Truncation of the N-terminal ectodomain has implications in the *N*-glycosylation and transport to the cell surface of Edg-1/S1P1 receptor. *J. Biochem.* **134,** 667–673
33. Biederbick, A., Kern, H. F., and Elsässer, H. P. (1995) Monodansylcadaverine (MDC) is a specific *in vivo* marker for autophagic vacuoles. *Eur. J. Cell Biol.* **66,** 3–14
34. Bligh, E. G., and Dyer, W. J. (1959) A rapid method of total lipid extraction and purification. *Can J. Biochem. Physiol.* **37,** 911–917
35. Okazaki, T., Bell, R. M., and Hannun, Y. A. (1989) Sphingomyelin turnover induced by vitamin D3 in HL-60 cells. Role in cell differentiation. *J. Biol. Chem.* **264,** 19076–19080
36. Kimura, S., Noda, T., and Yoshimori, T. (2007) Dissection of the autophagosome maturation process by a novel reporter protein, tandem fluorescent-tagged LC3. *Autophagy* **3,** 452–460
37. Kondo, T., Matsuda, T., Tashima, M., Umehara, H., Domae, N., Yokoyama, K., Uchiyama, T., and Okazaki, T. (2000) Suppression of heat shock protein-70 by ceramide in heat shock-induced HL-60 cell apoptosis. *J. Biol. Chem.* **275,** 8872–8879
38. Kondo, Y., Kanzawa, T., Sawaya, R., and Kondo, S. (2005) The role of autophagy in cancer development and response to therapy. *Nat. Rev. Cancer* **5,** 726–734
39. Mizushima, N., Levine, B., Cuervo, A. M., and Klionsky, D. J. (2008) Autophagy fights disease through cellular self-digestion. *Nature* **451,** 1069–1075
40. Mathew, R., Karantza-Wadsworth, V., and White, E. (2007) Role of au-

tophagy in cancer. *Nat. Rev. Cancer* **7,** 961–967
41. Kabeya, Y., Mizushima, N., Ueno, T., Yamamoto, A., Kirisako, T., Noda, T., Kominami, E., Ohsumi, Y., and Yoshimori, T. (2000) LC3, a mammalian homologue of yeast Apg8p, is localized in autophagosome membranes after processing. *EMBO J.* **19,** 5720–5728
42. Spassieva, S. D., Mullen, T. D., Townsend, D. M., and Obeid, L. M. (2009) Disruption of ceramide synthesis by CerS2 down-regulation leads to autophagy and the unfolded protein response. *Biochem. J.* **424,** 273–283
43. Huang, J., and Manning, B. D. (2008) The TSC1-TSC2 complex. A molecular switchboard controlling cell growth. *Biochem. J.* **412,** 179–190
44. Wullschleger, S., Loewith, R., and Hall, M. N. (2006) TOR signaling in growth and metabolism. *Cell* **124,** 471–484
45. Yang, Z., and Klionsky, D. J. (2010) Mammalian autophagy. Core molecular machinery and signaling regulation. *Curr. Opin. Cell Biol.* **22,** 124–131
46. Sato, K., Murata, N., Kon, J., Tomura, H., Nochi, H., Tamoto, K., Osada, M., Ohta, H., Tokumitsu, Y., Ui, M., and Okajima, F. (1998) Down-regulation of mRNA expression of Edg-3, a putative sphingosine 1-phosphate receptor coupled to Ca^{2+} signaling, during differentiation of HL-60 leukemia cells. *Biochem. Biophys. Res. Commun.* **253,** 253–256
47. Dobrowsky, R. T., Kamibayashi, C., Mumby, M. C., and Hannun, Y. A. (1993) Ceramide activates heterotrimeric protein phosphatase 2A. *J. Biol. Chem.* **268,** 15523–15530
48. Chalfant, C. E., Kishikawa, K., Mumby, M. C., Kamibayashi, C., Bielawska, A., and Hannun, Y. A. (1999) Long chain ceramides activate protein phosphatase-1 and protein phosphatase-2A. Activation is stereospecific and regulated by phosphatidic acid. *J. Biol. Chem.* **274,** 20313–20317
49. Bialojan, C., and Takai, A. (1988) Inhibitory effect of a marine-sponge toxin, okadaic acid, on protein phosphatases. Specificity and kinetics. *Biochem. J.* **256,** 283–290
50. Strum, J. C., Small, G. W., Pauig, S. B., and Daniel, L. W. (1994) 1-β-D-Arabinofuranosylcytosine stimulates ceramide and diglyceride formation in HL-60 cells. *J. Biol. Chem.* **269,** 15493–15497
51. Bose, R., Verheij, M., Haimovitz-Friedman, A., Scotto, K., Fuks, Z., and Kolesnick, R. (1995) Ceramide synthase mediates daunorubicin-induced apoptosis. An alternative mechanism for generating death signals. *Cell* **82,** 405–414
52. Blázquez, C., Salazar, M., Carracedo, A., Lorente, M., Egia, A., González-Feria, L., Haro, A., Velasco, G., and Guzmán, M. (2008) Cannabinoids inhibit glioma cell invasion by down-regulating matrix metalloproteinase-2 expression. *Cancer Res.* **68,** 1945–1952
53. Akao, Y., Kusakabe, S., Banno, Y., Kito, M., Nakagawa, Y., Tamiya-Koizumi, K., Hattori, M., Sawada, M., Hirabayasi, Y., Ohishi, N., and Nozawa, Y. (2002) Ceramide accumulation is independent of camptothecin-induced apoptosis in prostate cancer LNCaP cells. *Biochem. Biophys. Res. Commun.* **294,** 363–370
54. Ghosh, N., Patel, N., Jiang, K., Watson, J. E., Cheng, J., Chalfant, C. E., and Cooper, D. R. (2007) Ceramide-activated protein phosphatase involvement in insulin resistance via Akt, serine/arginine-rich protein 40, and ribonucleic acid splicing in L6 skeletal muscle cells. *Endocrinology* **148,** 1359–1366
55. Stratford, S., Hoehn, K. L., Liu, F., and Summers, S. A. (2004) Regulation of insulin action by ceramide. Dual mechanisms linking ceramide accumulation to the inhibition of Akt/protein kinase B. *J. Biol. Chem.* **279,** 36608–36615
56. Banno, Y., Takuwa, Y., Akao, Y., Okamoto, H., Osawa, Y., Naganawa, T., Nakashima, S., Suh, P. G., and Nozawa, Y. (2001) Involvement of phospholipase D in sphingosine 1-phosphate-induced activation of phosphatidylinositol 3-kinase and Akt in Chinese hamster ovary cells overexpressing EDG3. *J. Biol. Chem.* **276,** 35622–35628
57. Hahn-Windgassen, A., Nogueira, V., Chen, C. C., Skeen, J. E., Sonenberg, N., and Hay, N. (2005) Akt activates the mammalian target of rapamycin by regulating cellular ATP level and AMPK activity. *J. Biol. Chem.* **280,** 32081–32089
58. Krymskaya, V. P., and Goncharova, E. A. (2009) PI3K/mTORC1 activation in hamartoma syndromes. Therapeutic prospects. *Cell Cycle* **8,** 403–413
59. Krymskaya, V. P., Snow, J., Cesarone, G., Khavin, I., Goncharov, D. A., Lim, P. N., Veasey, S. C., Ihida-Stansbury, K., Jones, P. L., and Goncharova, E. A. (2011) mTOR is required for pulmonary arterial vascular smooth muscle cell proliferation under chronic hypoxia. *FASEB J.* **25,** 1922–1933
60. El-Naggar, S., Liu, Y., and Dean, D. C. (2009) Mutation of the Rb1 pathway leads to overexpression of mTOR, constitutive phosphorylation of Akt on serine 473, resistance to anoikis, and a block in c-Raf activation. *Mol. Cell. Biol.* **29,** 5710–5717
61. Deng, Q., Clemas, J. A., Chrebet, G., Fischer, P., Hale, J. J., Li, Z., Mills, S. G., Bergstrom, J., Mandala, S., Mosley, R., and Parent, S. A. (2007) Identification of Leu-276 of the S1P1 receptor and Phe-263 of the S1P3 receptor in interaction with receptor specific agonists by molecular modeling, site-directed mutagenesis, and affinity studies. *Mol. Pharmacol.* **71,** 724–735
62. Hla, T., Lee, M. J., Ancellin, N., Paik, J. H., and Kluk, M. J. (2001) Lysophospholipids. Receptor revelations. *Science* **294,** 1875–1878
63. Okajima, F., Tomura, H., Sho, K., Nochi, H., Tamoto, K., and Kondo, Y. (1996) Involvement of pertussis toxin-sensitive GTP-binding proteins in sphingosine 1-phosphate-induced activation of phospholipase C-Ca^{2+} system in HL60 leukemia cells. *FEBS Lett.* **379,** 260–264
64. Pettus, B. J., Kitatani, K., Chalfant, C. E., Taha, T. A., Kawamori, T., Bielawski, J., Obeid, L. M., and Hannun, Y. A. (2005) The coordination of prostaglandin E_2 production by sphingosine-1-phosphate and ceramide-1-phosphate. *Mol. Pharmacol.* **68,** 330–335
65. Liu, G., Burns, S., Huang, G., Boyd, K., Proia, R. L., Flavell, R. A., and Chi, H. (2009) The receptor S1P1 overrides regulatory T cell-mediated immune suppression through Akt-mTOR. *Nat. Immunol.* **10,** 769–777
66. Chang, C. L., Ho, M. C., Lee, P. H., Hsu, C. Y., Huang, W. P., and Lee, H. (2009) S1P(5) is required for sphingosine 1-phosphate-induced autophagy in human prostate cancer PC-3 cells. *Am. J. Physiol. Cell Physiol.* **297,** C451–458